Signal Transduction and Functional Imaging

Molecular Cancer Research

A Hypoxia-Inducible HIF1–GAL3ST1-Sulfatide Axis Enhances ccRCC Immune Evasion via Increased Tumor Cell–Platelet Binding

Claire M. Robinson[1,2], Betty P.K. Poon[1,2], Yoshihito Kano[1,2], Fred G. Pluthero[3], Walter H.A. Kahr[2,3,4], and Michael Ohh[1,2]

Abstract

Clear cell renal cell carcinoma (ccRCC) is the most common form of kidney cancer and the major cause of mortality for individuals with von Hippel-Lindau (VHL) disease. ccRCC is characterized most frequently by inactivation of VHL tumor suppressor protein that mediates degradation of the alpha subunit of the hypoxia-inducible factor (HIF) transcription factor family. HIF has been implicated in disease progression and the aim of this study was to identify novel HIF target genes that may contribute to ccRCC. We show that GAL3ST1, an enzyme that catalyzes the sulfonation of the plasma membrane sulfolipid sulfatide, is among the top 50 upregulated genes in ccRCC tissue relative to matched normal tissue. Increased expression of GAL3ST1 in primary ccRCC correlates with decreased survival. We show that GAL3ST1 is a HIF target gene whose expression is induced upon VHL loss leading to the accumulation of its enzymatic product sulfatide. Notably, platelets bind more efficiently to renal cancer cells with high GAL3ST1-sulfatide expression than to GAL3ST1-sulfatide–negative counterparts, which protects ccRCC cells against natural killer cell–mediated cytotoxicity. These results suggest that GAL3ST1 is a HIF-responsive gene that may contribute to ccRCC development via promoting cancer cell evasion of immune surveillance.

Implications: Cancer development is in part dependent on evasion of immune response. We identify a HIF target gene product GAL3ST1 that may play a role in this critical process.

Introduction

Renal cancer accounts for 2%–3% of all diagnosed cancers (1). Several distinct types of renal cancer exist including clear cell renal cell carcinoma (ccRCC), oncocytoma, chromophobe, and papillary cell RCC (PRCC). Of these, ccRCC is the most common, accounting for approximately 80% of all renal cancer cases (2). If it is diagnosed early enough the cancerous kidney is surgically removed. However, approximately one third of patients have locally advanced or metastatic cancer at diagnosis, and up to 30% of patients develop metastases during therapy. Advanced ccRCC, stages 3 and 4, have low survival rates with a 5-year survival rate of 53% and 8%, respectively.

Loss or mutation of von Hippel-Lindau (*VHL*) tumor suppressor gene is the most frequently occurring genetic aberration in sporadic ccRCC, evident in more than 60% of cases (3). Other mutations in sporadic ccRCC have been reported, predominantly of the genes controlling the epigenome, however these occur at a much lower frequency (3). A rare, hereditary, autosomal-dominant cancer syndrome called VHL disease also provides evidence of VHL involvement in ccRCC. VHL disease has several subcategories that depend on mutational status and relative risk of developing various tumor types including highly vascularized hemangioblastoma of the brain, spinal cord, or eye, and catecholamine secreting pheochromocytoma arising from the adrenal glands. The primary cause of mortality in patients with VHL is, however, due to the development of ccRCC, underscoring the importance of VHL mutation or loss in ccRCC (4).

VHL is the substrate-conferring component of E3 ubiquitin ligase. Multiple targets of VHL have been proposed but its involvement in the degradation of the alpha subunit of transcription factors called hypoxia-inducible factors (HIF), of which there are three (HIF1α, -2α, and -3α) in mammals, is the best described VHL target (5, 6). Under normal oxygen tension, HIFs are rapidly hydroxylated at two proline sites (HIF1α, P402 and P564; HIF2α, P405 and P531) within the oxygen-dependent degradation domain (ODD) by prolyl hydroxylases that utilize Fe^{2+}, 2-α-ketoglutarate, and O_2 to catalyze the prolyl-hydroxylation reaction (5, 7). If O_2 levels become limited or VHL is mutated or lost, HIFα is rapidly stabilized. HIFα forms a heterodimer with the constitutively expressed HIFβ and binds to the hypoxia-responsive

[1]Department of Laboratory Medicine & Pathobiology, University of Toronto, Toronto, Ontario, Canada. [2]Department of Biochemistry, University of Toronto, Toronto, Ontario, Canada. [3]Division of Haematology/Oncology and Cell Biology Program, Peter Gilgan Centre for Research and Learning, The Hospital for Sick Children, Toronto, Ontario, Canada. [4]Department of Paediatrics, University of Toronto, Toronto, Ontario, Canada.

Note: Supplementary data for this article are available at Molecular Cancer Research Online (http://mcr.aacrjournals.org/).

Corrected online April 2, 2021.

Corresponding Author: Michael Ohh, University of Toronto, Medical Science Building, Room 6306, 1 King's College Circle, Toronto, Ontario M5S 1A8, Canada. Phone: 416-946-7922; Fax: 416-978-5959; E-mail: michael.ohh@utoronto.ca

Mol Cancer Res 2019;17:2306–14

doi: 10.1158/1541-7786.MCR-19-0461

element (HRE; 5′-ACGTG-3′) to upregulate transcription of genes involved in adaptation to hypoxia, including those that promote angiogenesis (e.g., *VEGF*), glycolysis (e.g., *GLUT1*), and erythropoiesis (e.g., *EPO*).

The HRE sequence is a commonly occurring sequence within the genome and the current list of HIF target genes of which there are approximately 70 is not exhaustive (8). The best described HIF target genes promote survival, oxygen delivery, and a switch from oxidative phosphorylation to glycolysis. Many other genes have putative HREs, while HRE sequences are also found in other genomic locations where its function and the impact of HIF, if any, are unknown (9). In this study, we identified a gene called galactosylceramide sulfotransferase *(GAL3ST1* or *CST)* as a significantly upregulated gene in ccRCC patient tissue compared with matched normal tissue. We found that GAL3ST1 contains two putative HREs in its promoter making it a putative hypoxia-responsive gene. This enzyme promotes the synthesis of sulfatides by catalyzing the sulfonation of galactosylceramide and lactosylceramide to galactosylceramide sulfate (SM3) and lactosylceramide sulfate (SM4). Sulfatides (SM3 and SM4) are sulfoglycolipids that are multifunctional membrane-bound molecules involved in multiple cellular processes, including ligand binding, that are relevant to immune responses and hemostasis. They comprise a significant proportion of the myelin sheath of neuronal cells but are also reported to be upregulated in various cancer cells including in ccRCC (10). Given the presence of putative HREs in this gene's regulatory region, we hypothesized that this upregulation was a VHL-dependent, HIF-mediated event, which may account for the increased levels of sulfatides reported to be present in renal cancer cells (10). The aim of this study was to determine the mechanism of transcriptional upregulation of *GAL3ST1* in ccRCC and investigate the potential functional consequences of GAL3ST1-sulfatide in the pathogenesis of ccRCC.

Materials and Methods

Donor consent and platelet isolation

This study was performed according to the guidelines of the Research Ethics Board at The Hospital for Sick Children. Written informed consent was provided according to the Declaration of Helsinki. Washed platelets were prepared by centrifugation of citrated blood from healthy volunteers. Platelet rich plasma was removed and washed in sodium citrate PBS to prepare washed platelets.

Microarray and publically available datasets

The internal review board at the Van Andel Research Institute provided ethical approval for the use of diseased and normal human kidney samples. These were obtained from the Cooperative Human Tissue Network. The Affymetrix HG-U133 Plus 2.0 GeneChip platform was used to measure transcriptional changes in each sample. An extended version of this dataset is available in Supplementary Data 1. ChIP Atlas (http://chip-atlas.org) was used to investigate HIF binding to GAL3ST1 in a variety of renal cell lines (11). Datasets from Smythies and colleagues (ref. 12; Gene Expression Omnibus accession #GSE120885) were analyzed using integrative genome viewer.

Cell culture and reagents

Cell lines (786-O, RCC4, HEK293A, HEK293T, and NK-92) were purchased from American Type Culture Collection (ATCC). With the exception of NK-92 cells, cells were cultured in DMEM (Wisent Bio Products) supplemented with 10% foetal calf serum and penicillin-streptomycin. NK-92 cells were cultured, according to the manufacturer's instructions, in MEM supplemented with 100 U/mL IL-2. 786-MOCK, 786-VHL, 786-VHL_C162F, 786-VHL_ L188V, RCC4-MOCK and RCC4-VHL were cultured in DMEM supplemented with FBS, penicillin streptomycin and 250 mg/mL G418.

Unless otherwise specified, cells were cultured at 37°C in a humidified incubator with 5% CO2. A hypoxic incubator was used to grow cells in 1% O2.

Generation of stable cell lines

Stable cell lines were generated using the pGIPZ-turboGFP lentiviral vector containing an shSCR (Open Biosystems) or an shGAL3ST1 (a gift from Dr. Meredith Irwin, The Hospital for Sick Children, Toronto, Ontario, Canada). Stable polyclonal cell lines using both lentiviruses were generated in both 786-O and RCC4 cells. Cells were selected using puromycin and stable cells were continually grown in low dose puromycin for the duration of their time in culture.

Western blotting

To identify differences in protein expression, western blotting was performed. Protein lysates were separated by size on a SDS-PAGE gel. Following transfer onto PVDF membrane, membranes were blocked and then incubated with primary antibodies selective for proteins of interest. Following primary antibody incubation, membranes were washed, incubated with HRP conjugated secondary antibodies and then washed again before developing. The following primary antibodies were used for detection of proteins using western blot. Anti-GAL3ST1 and anti-GLUT1 (Abcam), rabbit anti-HA (C29F4; Cell Signaling Technology), anti-HIF2a and anti-HIF1a (H1alpha67) (Novus Biologicals), anti-HIF1a antibody (54/HIF-1a; BD Transduction Laboratories), anti-vinculin (V284; Upstate), anti-b-actin (AC-74; Sigma-Aldrich). Secondary horse radish peroxidase conjugated antibodies were anti-mouse IgG and anti-rabbit IgG (Pierce Thermo Scientific).

RNA extraction, cDNA synthesis, and qPCR

The RNeasy Mini Kit (Qiagen) was used to extract RNA. RNA was quantified using nanodrop and equal amounts of RNA sample was used to generate cDNA using manufactures instructions (Invitrogen). cDNA was used for quantitative PCR using SYBR Green (Sigma). NCBI/Primer-BLAST (http://www.ncbi.nlm.nih.gov/tools/primer-blast/) was used to generate primer sequences that would specifically detect genes of interest. Analysis of qPCR results were preformed using the 2–ΔΔCtmethod and β-Actin was used as the housekeeping gene.

Primer sequences used for qPCR are as follows; GAL3ST1-F, 5′-AGCGGCACAGTCATGGCTCA-3′; GAL3ST1-R, 5′-AGCATCTCAGACACCAGGCGTG-3′; GLUT1-F, 5′-CACCACCTCACTCCTGTTACTT-3′; GLUT1-R, 5′-CAAGCATTTCAAAACCATGTTTCTA-3′; b-ACTIN-F, 5′-AAAGCCACCCCACTTCTCTCTAA-3′; b-ACTIN-R, 5′-ACCTCCCCTGTGTGGACTTG-3′.

Transient reverse transfection and siRNA-mediated knockdown

Plasmids were transiently transfected into cells using Polyethylenimine transfection reagent. Cells were harvested 48 hours after transfection. For siRNA-mediated knockdown, ON-TARGET plus SMART pool siRNAs against HIF1α (siHIF1α), HIF2α (siHIF2α), or scrambled non-targeting RNA (siSCR) were all obtained from Dharmacon.

Luciferase assays and plasmids

The GAL3ST1 promoter was cloned into pGL3-luciferase promoter vector (Promega). Putative hypoxic response elements were mutated in wild-type GAL3ST1 using site directed mutagenesis to generate pGL3-GAL3ST1mutHRE1, pGL3-GAL3ST1mutHRE2 and pGL3-GAL3ST1mutHRE1+HRE2. The Dual Luciferase Reporter Assay System (Promega) was then used to preform luciferase assays. HEK293 cells were transfected with luciferase plasmids alongside either pcDNA3-EMPTY, pcDNA3-HA-HIF1α (P>A), or pcDNA3-HAHIF2α (P>A). The degree of promoter activity was quantified by measuring luciferase activity that was normalized to protein concentration.

Chromatin Immunoprecipitation (ChIP)

ChIP was performed to interrogate the degree of HIF1α or HIF2α binding to HREs DNA was cross-linked and fragmented. Antibodies specific for HIF1α and HIF2α (Novus Biologicals) were used to immunoprecipitate fragmented DNA. Immunoprecipitated DNA was purified and quantified using qPCR. The following primers were used to detect HIF binding: GAL3ST1(HRE2)-F, 5′-TCCTGTCTCCCAGTGATCGCAGAG-3′; GAL3ST1(HRE2)-R, 5′-TTCTACCCACTGCCTGAGCCACG-3′; GAL3ST1(internal)-F, 5′-TTTCCTGGCCTCAGGGGCCC-3′; GAL3ST1(internal)-R, 5′-GAGGGCCTTCCCACCTCCCC-3′; and b-ACTIN-F, 5′-AGCGTGCGCCGTTCCGAAAG-3′; b-ACTIN-R, 5′-TGGGTTTTATAGGGCGCCGCC-3'.

Immunofluorescence

Cells were grown on glass coverslips and treated as indicated. After treatment, cells were fixed with 4% paraformaldehyde, washed, and blocked with 10% FBS. Fixed cells were incubated in primary antibodies specific for the protein of interest. These were anti-SM3/SM4 sulfatide antibody (Millipore) or rabbit anti-HA (C29F4; Cell Signaling Technology). This was followed by incubation with fluorescently conjugated secondary antibodies, either rhodamineconjugated anti-mouse IgG and anti-rabbit IgG secondary (Pierce Thermo Scientific) and Alexa Fluor 488–conjugated anti-mouse IgG (Invitrogen). Nuclei were stained with DAPI. Following the staining protocol, coverslips were mounted with VectaShield Mounting Medium (Vector Laboratories) and imaged using an Axioplan2 imaging microscope and Axiocam HRM Digital Camera (Carl Zeiss Canada Ltd.).

Cells examined for platelet adhesion were stained with wheat germ agglutinin conjugated with Alexa Fluor 555 and Actin Green (both from Life Technologies) according to the manufacturer's instructions. Nuclear DNA was stained with Hoechst 33258 (Sigma-Aldrich). Cells were rinsed, mounted with Dako fluorescent medium, and imaged using a Quorum spinning disk laser fluorescence microscope with a 60 × oil immersion objective. Images were prepared using Bitplane Imaris 8.0 and Adobe Photoshop.

Natural killer cell cytotoxic assays

Renal cancer cells were coincubated with NK-92 cells at 37°C for 3 hours in the absence or presence of platelets. Post-incubation, cells were kept on ice, stained with annexin V and 7-AAD, and analyzed using flow cytometry.

Flow cytometry

For flow cytometry, the following dyes and antibodies were used: Calcein AM (eBioscience, 65-0853-39), Calcein Red (ATT Bioquest, 21900), Annexin V Alexa Fluor 647 conjugate (Invitrogen, A23204), 7-Aminoactinomycin D (Invitrogen, A1310), and PE anti-human CD41 (BioLegend, 303706).

Statistical analysis

Experiments were repeated a minimum of three times. Statistical analysis was performed using Prism where statistical tests were applied. Where appropriate, *t* tests or one-way ANOVA with *post hoc* Tukey test were used to determine the significance between samples.

Results

GAL3ST1 expression is upregulated in ccRCC

A tissue microarray was used to quantify mRNA expression in 10 different primary RCC tumors and matched normal tissue. Expression values for all RCC samples were averaged and ranked from highest to lowest. *GAL3ST1* expression ranked within the top 50 highest-expressed genes in these primary tumor samples (Table 1). *GAL3ST1* was identified as a gene of interest as unlike many of the other genes listed, there is no known role for GAL3ST1 in ccRCC. In publically available datasets generated from patients with renal cancer (www.proteinatlas.org; ref. 13), high *GAL3ST1* mRNA level was unfavorable for disease outcome ($P < 0.001$; Fig. 1), suggesting a role for *GAL3ST1* in disease progression. Expression data from a tissue microarray was used to quantify *GAL3ST1* mRNA expression in human renal cancer specimens of the following subtypes; ccRCC, chromophobe RCC, oncocytoma, type I PRCC, and type II PRCC. *GAL3ST1* expression was significantly higher in ccRCC than in other subtypes when compared with expression in normal tissue (see Fig. 2.1A in ref. 14; a more comprehensive version of this dataset is available in Supplementary Fig. S1). Concordantly, GAL3ST1 protein level was markedly upregulated in six primary ccRCC tissue specimens compared with matched normal tissues (see Fig. 2.1C in ref. 14). Expression of a well-established HIF target GLUT1 (*SLC2A1*) was upregulated in ccRCC samples and served as a positive control (see Fig. 2.1C in ref. 14).

GAL3ST1 is a HIF target gene

Analysis of human renal tumor subtypes for *GAL3ST1* demonstrated that this gene was upregulated in ccRCC (see Fig. 2.1A in ref. 14). We therefore hypothesized that its upregulation may be dependent on VHL loss, an event specific and frequent to ccRCC. *GAL3ST1* mRNA expression in renal cancer cell lines 786-MOCK

Table 1. A list of the most upregulated genes in 10 ccRCC samples compared with normal kidney

Rank	Gene ID	Gene symbol
1	54901	NDUFA4L2
2	84634	KISS1R
3	7130	TNFAIP6
4	4885	NPTX2
5	1573	CYP2J2
6	2173	FABP7
7	51129	ANGPTL4
8	112399	EGLN3
9	100133188	NA
10	5169	ENPP3
.....	.....	.....
42	1520	CTSS
43	9514	GAL3ST1
44	714	C1QC

NOTE: Gene expression in 10 primary ccRCC tumor samples was analyzed by Affymetrix microarray; GEO accession #GDS1344. Averages were measured across all 10 samples and ranked from highest to lowest (see top 50 list in Table 2.1 in ref. 14).

and RCC4-MOCK, as well as their counterparts stably expressing HA-VHL (786-VHL and RCC4-VHL) was quantified. In all cell types tested, *GAL3ST1* was repressed when VHL was reexpressed in these cells, similar to HIF-regulated gene *GLUT1*, which was used as a positive control (see Fig. 2.2A in ref. 14). Intriguingly, when we tested protein expression in 786 cells stably expressing a VHL mutant capable of degrading HIFα (VHL-L188V), GAL3ST1 was repressed, whereas in cells lacking or expressing a mutant VHL incapable of degrading HIF (VHL-C162F), GAL3ST1 was upregulated (see Fig. 2.2C in ref. 14). *GAL3ST1* expression was higher in 786-VHL and RCC4-VHL cells maintained in hypoxia than in normoxia, similar to the *bona fide* hypoxic-responsive gene *GLUT1* (see Fig. 2.3A in ref. 14). Furthermore, hypoxia-mediated stabilization of HIFα was associated with increased GAL3ST1 protein expression in RCC4-VHL cells (see Fig. 2.3C in ref. 14), and siRNA-mediated knockdown of both HIF1α and HIF2α in RCC4-MOCK cells decreased GAL3ST1 expression (see Fig. 2.3E,F in ref. 14), suggesting HIF-dependent transcription of *GAL3ST1*. HIF1 and HIF2 bind to a HRE with the following sequence 5′-[A/G]CGTG-3′. The *GAL3ST1* promoter contains two putative HREs (HRE1 and HRE2; see Fig. 2.4B in ref. 14). HRE1 is situated within the 5′-UTR of *GAL3ST1* and HRE2 is located approximately 800 bp upstream of the first. This region, containing both putative HREs, was subcloned into pGL3-luciferase vector (pGL3-GAL3ST1). Site-directed mutagenesis was used to mutate one or both of the HRE sites (pGL3-GAL3ST1mutHRE1, pGL3-GAL3ST1mutHRE2, and pGL3-GAL3ST1mutHRE1+2). Stable HIF1/2-expressing plasmids with a proline to alanine (P>A) substitution mutation in the ODD (pcDNA3-HA-HIF1α-P>A or pcDNA3-HA-HIF2α-P>A) were cotransfected into cells and relative light units measured. These results demonstrated that HRE2 was responsible for HIF-mediated *GAL3ST1* expression (see Fig. 2.4E in ref. 14). ChIP experiments for either HIF1α or HIF2α demonstrated that both HIF1α and HIF2α bind to HRE2 in RCC4-VHL cells grown in hypoxic conditions (see Fig. 2.4F in ref. 14). Interrogation of publically available ChIP-seq datasets for HIF1, HIF2, and ARNT supported these findings (Supplementary Figs. S1 and S2).

GAL3ST1 expression leads to enhanced levels of sulfatides in the cell membrane of ccRCC cells

GAL3ST1 is involved in sulfatide biosynthesis by catalyzing the sulfonation of galactosylceramide and lactosylceramide to SM3 and SM4. Immunofluorescence was used to examine expression of sulfatides in 786-MOCK and 786-VHL, and RCC4-MOCK and RCC4-VHL. To directly compare levels of sulfatides between MOCK versus VHL cell types, 786-MOCK and 786-VHL, or RCC4-MOCK and RCC4-VHL, cells were seeded as mixed populations. In 786 cells, sulfatide levels (green) were negligible in cells expressing VHL (red), whereas sulfatide levels were high in VHL-null cells (see Fig. 2.3D in ref.

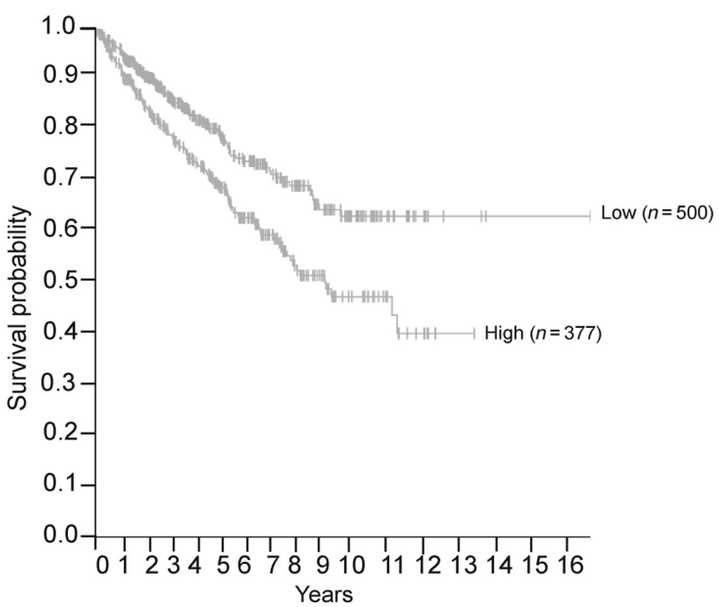

Figure 1.
GAL3ST1 expression is upregulated in ccRCC. Patients were separated into two groups based on FPKM value for *GAL3ST1*. Kaplan–Meier estimator measured survival outcomes in patients expressing high or low *GAL3ST1* mRNA and outcomes of the two groups were compared with log-rank tests [log-rank $P = 1.79e\text{-}4$ (prognostic, unfavorable)].

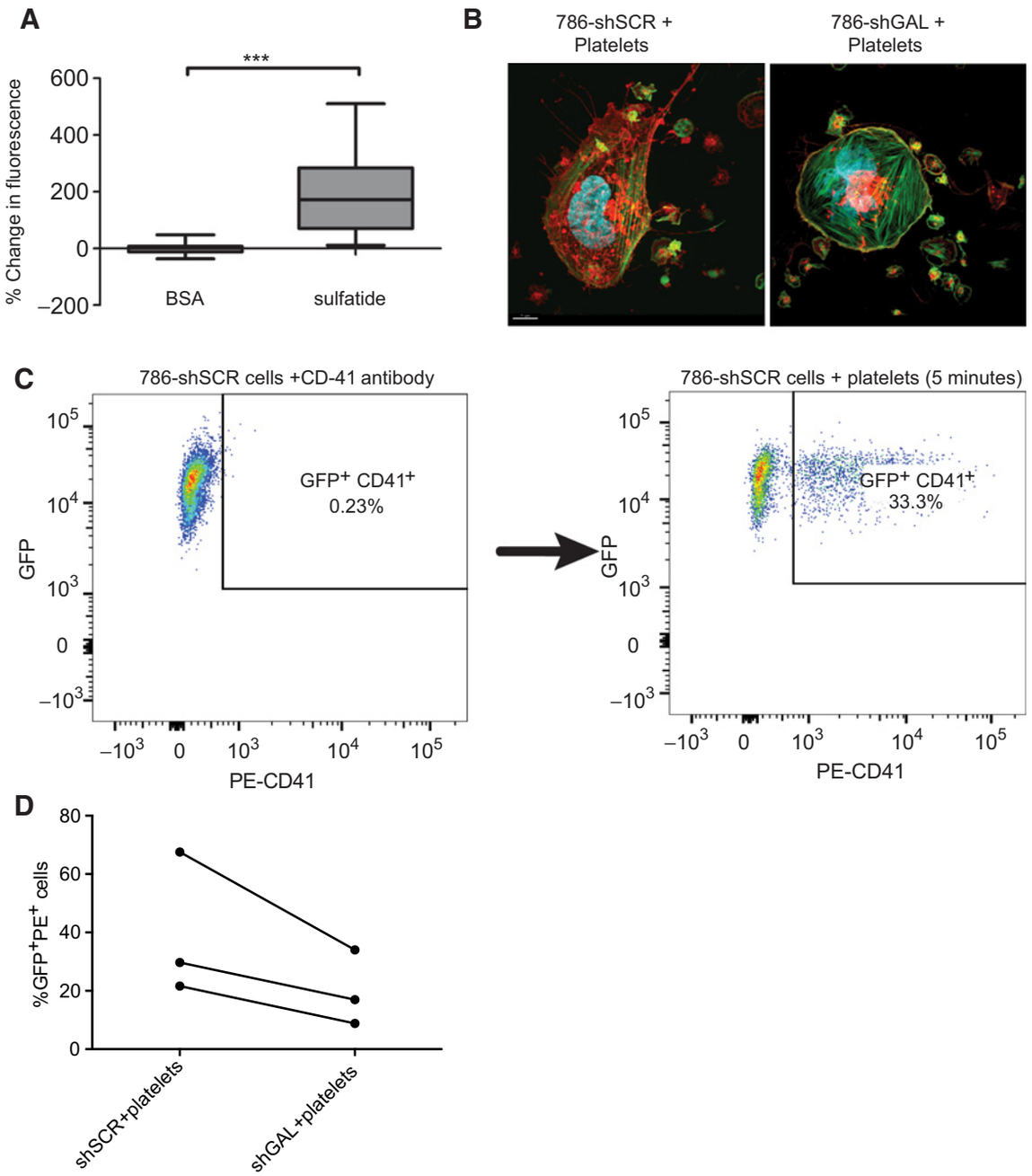

Figure 2.

Sulfatides promote platelet binding to cancer cells. **A,** Wells of a 96-well plate were coated with 2 μg/mL BSA or bovine sulfatides. Washed human platelets from healthy donors were stained with calcein AM and incubated in the coated wells. Following washes, florescence was measured using a fluorescent plate reader. Results are presented as a percent change in fluorescence of control (BSA). Data were analyzed using unpaired Student *t* test where, ***, $P < 0.001$. **B,** 786-shSCR and 786-shGAL were coincubated with human platelets from healthy donors stained with wheat germ agglutinin (red). Actin (green) stained both cells and activated platelets, while nuclei were stained with Hoechst (blue). **C,** An example of flow cytometry data acquired demonstrating the emergence of a double-positive cell population. Platelets were coincubated with GFP^+ renal cancer cells for 5 minutes. Samples were fixed, stained with PE-CD41, and analyzed using flow cytometry. **D,** The percentage of a GFP^+ $PE\text{-}CD41^+$ population was graphed for each platelet donor tested ($n = 3$).

14). In support of a role for HIF in sulfatide regulation, 786-VHL cells in hypoxia stained positive for sulfatide. A similar trend was apparent in RCC4-MOCK and RCC4-VHL cells grown in normoxia and hypoxia. To discern whether this was a GAL3ST1-mediated process, GAL3ST1 was stably knocked down using shRNA. In cell lines expressing scrambled shRNA

(786-pGIPZ-shSCR and RCC4-pGIPZ-shSCR), the expression of sulfatides was high, while this was lost upon stable knockdown of GAL3ST1 (786-pGIPZ-shGAL3ST1 and RCC4-pGIPZ-shGAL3ST1), demonstrating GAL3ST1 dependent regulation of sulfatide expression (see Fig. 2.5B in ref. 14). Efficient knockdown of GAL3ST1 in both cell lines was confirmed by Western blot analysis (see Fig. 2.5A in ref. 14).

Sulfatides promote platelet binding to cancer cells

Sulfatides on cancer cells have been proposed elsewhere as important in the metastatic process (15). One important aspect of this process is hematogenous dissemination, whereby cancer cells travel in the bloodstream to migrate to a new region (16), most often the lungs, bone, lymph nodes, liver, adrenal glands, and brain in ccRCC (17). During this process, immune cells should recognize and destroy cancer cells. However, cancer cells have developed mechanisms to evade such immune recognition. One such mechanism involves platelets, which are thought to shield circulating tumor cells from immune surveillance (18). We hypothesized that this may be a mechanism through which GAL3ST1-sulfatides promotes ccRCC metastasis. We tested whether platelets had the capacity to bind to sulfatides and showed that fluorescently labeled platelets bind more to sulfatide-coated wells than to wells coated with BSA (Fig. 2A). Immunofluorescence demonstrated the capacity of both 786-shSCR and 786-shGAL3ST1 cells to activate platelets and revealed classic morphologic changes associated with platelet activation (Fig. 2B). This imaging also clearly highlighted the capacity of platelets to bind to cancer cells (Fig. 2B). To quantify platelet binding to GFP^+ 786-shSCR and 786-shGAL3ST1 cells, we used flow cytometry and PE-CD41 antibody to label healthy donor washed human platelets. We observed the emergence of a double-positive population following coincubation of platelets with renal cancer cells (Fig. 2C). This was significantly different after 5 minutes of coincubation in 786-shSCR versus 786-shGAL3ST1 cells with approximately 50% more double positives in the 786-shSCR population, suggesting increased binding of platelets to 786-shSCR (sulfatide high) cells than 786-shGAL3ST1 (sulfatide low) cells (Fig. 2D).

Platelets protect GAL3ST1-sulfatide–expressing cells from natural killer cell–mediated destruction

Platelet binding to 786-shSCR cells was more robust than to 786-shGAL3ST1 cells (Fig. 2D). We next interrogated *in vitro* whether this binding had any impact on immune cell activity. The natural killer (NK) cell line, NK-92, was used as a representative NK cell. RCC cells were incubated alone, with NK-92 cells, or with platelets and NK-92 cells. Cell death was quantified using flow cytometry as annexin V and/or $7AAD^+$ cells (Fig. 3A). GFP^+ 786-shSCR cells were significantly protected from NK-mediated cell death compared with GFP^+ 786-shGAL3ST1 cells, suggesting that the protection conferred to cancer cells by platelets is at least in part mediated by GAL3ST1-sulfatides (Fig. 3B). 786-shGAL3ST1 cells had approximately 5%–10% more dead cells than 786-shSCR cells when incubated in the presence of NK-92 cells and platelets (Fig. 3C). Interestingly, when the platelet activator, U46619, was used to maximally activate platelets preincubation, platelets protected both cell types against NK-92 cell cytotoxicity than cancer cell–induced platelet activation alone (Fig. 3D). These results support a model whereby platelet–sulfatide interactions promote the evasion of cancer cells from immune cell surveillance and killing; a protection that is significantly compromised upon loss or reduction of GAL3ST1 expression (Fig. 4).

Discussion

This study demonstrates that *GAL3ST1* is a novel HIF-mediated gene that can be upregulated by both HIF1α and HIF2α as a consequence of VHL loss or hypoxia. We show that GAL3ST1 regulates sulfatide levels and demonstrate a potential role for GAL3ST1-sulfatides in cancer cell–platelet interactions that may promote immune cell evasion. Our study has focused on ccRCC where high levels of sulfatides have previously been reported (19). However, high sulfatide expression is not exclusive to this tumor type. Studies in pulmonary adenocarcinoma, breast, ovarian, and colon cancer have all reported changes in sulfatide levels (20–23). Interestingly HIF1α and/or HIF2α are often stabilized in these cancers and based on the findings of this study it is likely that *GAL3ST1* may be upregulated via HIF-mediated transcription in other tumor types. Others have previously reported that increased GAL3ST1 expression in renal cancer is mediated by a variety of cytokines (24, 25) including TGFα (26), a gene that can be upregulated by HIF (27).

We found that increased *GAL3ST1* is predictive of poor outcome in ccRCC. However, the precise contribution of GAL3ST1 to cancer initiation and/or progression is unclear. A recent study has described a role for the enzyme GAL3ST1 in a primary tumor setting (23). Here, the authors provided evidence that upregulation of GAL3ST1 decreased primary tumor growth via reduction of galactosylceramide levels that then increased susceptibility of cells to stress-induced apoptosis (23). In contrast, the same study suggested that this pathway was oncogenic in metastatic cancer where GAL3ST1-sulfatide was implicated in promoting disease progression (23). It is interesting to note that in basal breast cancer cells inhibition of UGT8, an enzyme upstream of GAL3ST1 resulted in decreased tumor growth in xenografts (28). While in another study, overexpression of GAL3ST1 in hepatocellular carcinoma cells resulted in increased intrahepatic metastasis (29). Thus, while these studies point toward an oncogenic role for GAL3ST1-sulfatides in a metastatic setting, the role of this pathway in primary tumors requires more investigation.

In the 1860s, Armand Trousseau first described a syndrome that involved repeated vessel inflammation due to blood clots as an early sign of cancer. This became known as "The Trousseau Sign of Malignancy." Trousseau suspected that the syndrome was not because of an inflammatory stimulus but due to the hyper-coagulation ability of the underlying cancer. Since then, high platelet counts (thrombocytosis) have been proposed as an independent determinant of ccRCC and some have suggested this as a biomarker of the disease (30). Platelets may enhance oncogenesis via various mechanisms, which have been described in detail elsewhere (31). But, perhaps the most compelling evidence of platelet promotion of oncogenesis is that pharmacologic induction of thrombocytopenia in mouse models of metastatic cancer significantly reduces

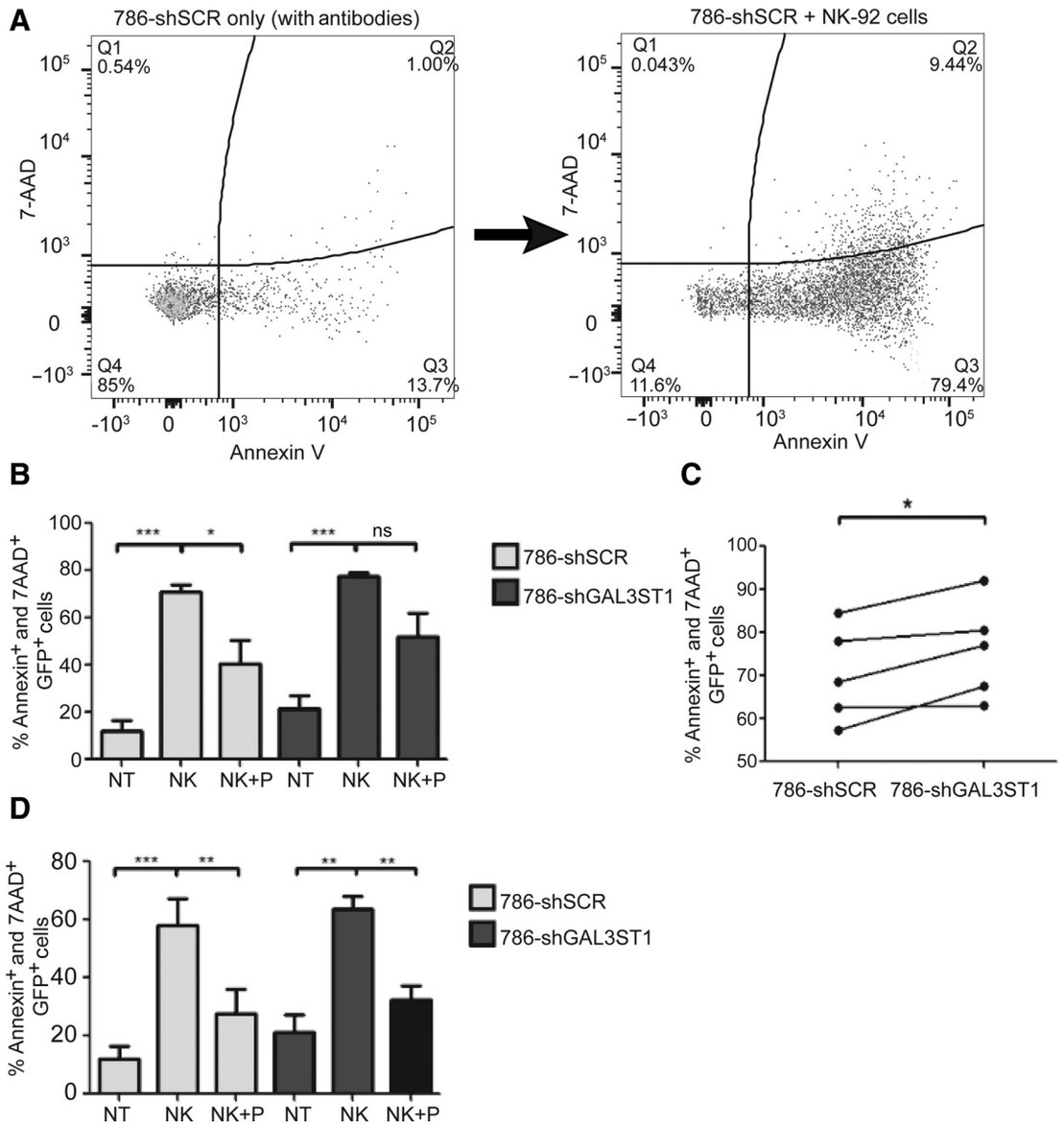

Figure 3.

Platelets protect GAL3ST1-sulfatide–expressing cells from NK cell–mediated destruction but not GAL3ST1-sulfatide–negative cells. NK-92 cells were stained with Calcein-Red. 786-shSCR or -shGAL3ST1 are GFP$^+$. Cancer cells were incubated for 3 hours in the presence or absence of NK-92 cells ± washed healthy platelets. After incubations, cells were stained for 7-AAD and Annexin V and cell death was quantified using flow cytometry. **A,** An example of the gating regime applied to the experiments presented and the significant shift in AnnexinV$^+$ cells upon coincubation of ccRCC cells with NK-92 cells. A total of 10,000 events were recorded for each experiment. **B,** Cell death in 786-shSCR and 786-shGAL3ST1 cells coincubated in the presence or absence of platelets (P) or NK-92 cells (NK). Untreated cancer cells are presented in the figure as NT. $n = 5$ with washed human platelets from 5 healthy donors. **C,** NK-mediated cell death in samples coincubated with platelets in 786-shSCR and 786-shGAL3ST1 cells. A paired *t* test was used to evaluate significance between the groups where $n = 5$ healthy donors. **D,** Using the same experimental setup, platelets were activated with U46619 and then coincubated with shSCR or shGAL3ST1 ± NK-92 cells. In figures **B** and **D,** a one-way ANOVA with *post hoc* Tukey test was applied to determine statistical significance (*, $P < 0.05$; **, $P < 0.01$; ***, $P < 0.001$; ns, not significant).

tumor burden (32). In our study we demonstrate a strong interaction between GAL3ST1-sulfatide–positive ccRCC cells and platelets, which *in vitro* significantly protects cancer cells from NK cell–mediated death.

The enzymatic product of GAL3ST1, sulfatide, is best known as a constituent of the myelin sheath of neuronal cells, although sulfatides are also abundant in the kidney, gastrointestinal tract, and islets of Langerhans. In addition to upregulation in cancer, dysregulated sulfatides have been reported in other diseases (33). Interestingly in the kidney, sulfatides have been suggested as important for adaptation to metabolic acidosis, a feature of hypoxemia (34). However, its multiple roles

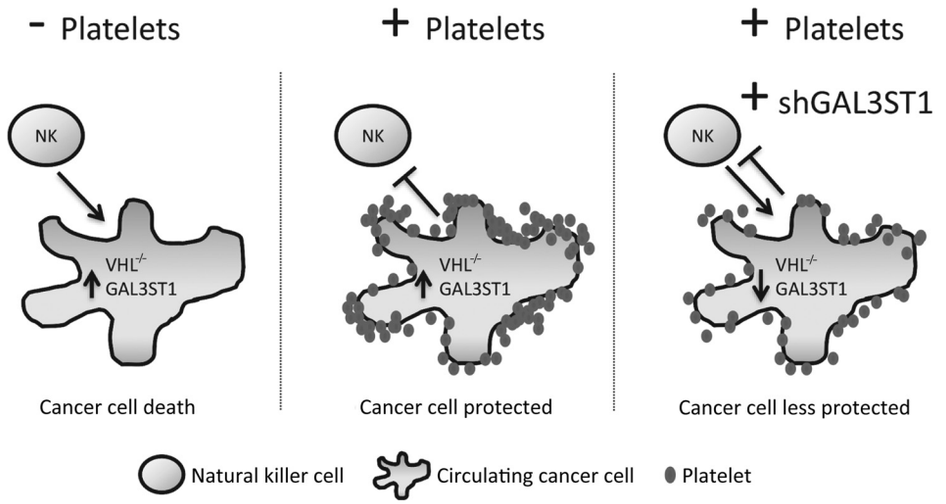

Figure 4.
Model of GAL3ST1 in NK cell–mediated tumor cell killing. $VHL^{-/-}$ renal cancer cells express high levels of GAL3ST1 and NK cells can target these cells for destruction (left). In the presence of platelets that interact with $VHL^{-/-}$ cells, NK cells have significantly restricted abilities to target renal cancer cells for destruction (middle). When GAL3ST1 expression is decreased, platelet interactions with renal cancer cells are perturbed and NK-mediated killing is increased (right).

and importance in disease is primarily due to the fact that sulfatides act as ligands for many cell adhesion molecules including laminin, fibronectin, selectins, von-Willebrand factor (VWF), and various integrins. These observations led us to focus on the contribution of GAL3ST1-sulfatides to the metastatic arm of ccRCC, specifically during hematogenous dissemination. We demonstrate that platelets bind more rapidly to cells with GAL3ST1-sulfatides than to cells that do not express GAL3ST1-sulfatides. This is in support of a recent study that demonstrated the ability of platelets to interact with breast cancer cells with high levels of sulfatides, while platelets interacted less with breast cancer cells expressing low levels of sulfatides (23). There are various mechanisms through which this may occur. P-selectin (CD62P) is found in α-granules of platelets. Upon platelet activation, P-selectin in α-granules relocates to the surface of platelets. Sulfatide has been proposed as a ligand for P-selectin in cancer cells (35), including murine colon carcinoma cells and human hepatoma cells (15) and this may also be the case in our cell system. Intriguingly, in a murine colon carcinoma model, P-selectin–knockout mice had smaller primary tumors and decreased metastatic burden compared with WT mice (36). In this study the authors provided evidence of rosetting of WT mouse platelets around tumor cells that was also evident *in vivo* and thought to promote seeding of cancer cells to the lung. The frequency of these observations was significantly reduced in P-selectin–knockout mice (36). Others have alluded to a role for VWF, an important factor for platelet adhesion at wound sites. VWF is a sulfatide ligand and it has been reported that platelet binding to sulfatide can occur via VWF (37). The presence of sulfatides can also act to upregulate integrins such as αvβ3 and αvβ5 on tumor cells (28, 29, 38). Notably, activated αvβ3 on cancer cells have been shown to promote platelet interaction that promotes metastasis (39). Thus, there are likely a variety of mechanisms by which GAL3ST1-sulfatides promote ccRCC development and progression.

In conclusion, our study has revealed a novel HIF target gene that is upregulated upon VHL loss or hypoxia in ccRCC cells. GAL3ST1 expression impacts sulfatide levels in renal cancer cells. Although the GAL3ST1-sulfatides may have multiple functional consequences, we provide evidence of its interaction with platelets that promotes cancer cell evasion of NK-mediated cytotoxicity, a potentially important event during cancer development and progression.

Disclosure of Potential Conflicts of Interest

No potential conflicts of interest were disclosed.

Authors' Contributions

Conception and design: C.M. Robinson, M. Ohh
Development of methodology: C.M. Robinson, B.P.K. Poon, Y. Kano, W.H.A. Kahr
Acquisition of data (provided animals, acquired and managed patients, provided facilities, etc.): C.M. Robinson, B.P.K. Poon, F.G. Pluthero, W.H.A. Kahr
Analysis and interpretation of data (e.g., statistical analysis, biostatistics, computational analysis): C.M. Robinson, B.P.K. Poon, F.G. Pluthero
Writing, review, and/or revision of the manuscript: C.M. Robinson, W.H.A. Kahr, M. Ohh
Administrative, technical, or material support (i.e., reporting or organizing data, constructing databases): C.M. Robinson, B.P.K. Poon, Y. Kano
Study supervision: M. Ohh

Acknowledgments

We thank members of the Ohh laboratory for critical comments and discussions and Samantha Greer for her assistance with the GAL3ST1 analysis. We also thank staff at the Department of Immunology Flow Cytometry Facility, University of Toronto (Toronto, Canada) for their insight and guidance. This work was supported by funds from the Canadian Institutes of Health Research.

The costs of publication of this article were defrayed in part by the payment of page charges. This article must therefore be hereby marked *advertisement* in accordance with 18 U.S.C. Section 1734 solely to indicate this fact.

Received May 1, 2019; revised July 9, 2019; accepted August 14, 2019; published first August 19, 2019.

References

1. Ferlay J, Soerjomataram I, Dikshit R, Eser S, Mathers C, Rebelo M, et al. Cancer incidence and mortality worldwide: sources, methods and major patterns in GLOBOCAN 2012. Int J Cancer 2015;136:E359–86.
2. Hsieh JJ, Purdue MP, Signoretti S, Swanton C, Albiges L, Schmidinger M, et al. Renal cell carcinoma. Nat Rev Dis Primers 2017;3:17009.
3. Cancer Genome Atlas Research Network. Comprehensive molecular characterization of clear cell renal cell carcinoma. Nature 2013;499:43–9.
4. Kaelin WG Jr. Molecular basis of the VHL hereditary cancer syndrome. Nat Rev Cancer 2002;2:673–82.
5. Ivan M, Kondo K, Yang H, Kim W, Valiando J, Ohh M, et al. HIFalpha targeted for VHL-mediated destruction by proline hydroxylation: implications for O2 sensing. Science 2001;292:464–8.
6. Ohh M, Park CW, Ivan M, Hoffman MA, Kim TY, Huang LE, et al. Ubiquitination of hypoxia-inducible factor requires direct binding to the beta-domain of the von Hippel-Lindau protein. Nat Cell Biol 2000;2: 423–7.
7. Jaakkola P, Mole DR, Tian YM, Wilson MI, Gielbert J, Gaskell SJ, et al. Targeting of HIF-alpha to the von Hippel-Lindau ubiquitylation complex by O2-regulated prolyl hydroxylation. Science 2001; 292:468–72.
8. Wenger RH, Stiehl DP, Camenisch G. Integration of oxygen signaling at the consensus HRE. Sci STKE 2005;2005:re12.
9. Schodel J, Oikonomopoulos S, Ragoussis J, Pugh CW, Ratcliffe PJ, Mole DR, et al. High-resolution genome-wide mapping of HIF-binding sites by ChIP-seq. Blood 2011;117:e207–17.
10. Sakakibara N, Gasa S, Kamio K, Makita A, Nonomura K, Togashi M, et al. Distinctive glycolipid patterns in Wilms' tumor and renal cell carcinoma. Cancer Lett 1991;57:187–92.
11. Oki S, Ohta T, Shioi G, Hatanaka H, Ogasawara O, Okuda Y, et al. ChIP-Atlas: a data-mining suite powered by full integration of public ChIP-seq data. EMBO Rep 2018;19:pii: e46255.
12. Smythies JA, Sun M, Masson N, Salama R, Simpson PD, Murray E, et al. Inherent DNA-binding specificities of the HIF-1α and HIF-2α transcription factors in chromatin. EMBO Rep 2019;20:pii: e46401.
13. Uhlen M, Zhang C, Lee S, Sjöstedt E, Fagerberg L, Bidkhori G, et al. A pathology atlas of the human cancer transcriptome. Science 2017;357:pii: eaan2507.
14. Greer SN. Role of GAL3ST1 in renal cell carcinoma. University of Toronto 2012; http://hdl.handle.net/1807/33225.
15. Garcia J, Callewaert N, Borsig L. P-selectin mediates metastatic progression through binding to sulfatides on tumor cells. Glycobiology 2007;17: 185–96.
16. Chambers AF, Groom AC, MacDonald IC. Dissemination and growth of cancer cells in metastatic sites. Nat Rev Cancer 2002; 2:563–72.
17. Bianchi M, Sun M, Jeldres C, Shariat SF, Trinh QD, Briganti A, et al. Distribution of metastatic sites in renal cell carcinoma: a population-based analysis. Ann Oncol 2012;23:973–80.
18. Nieswandt B, Hafner M, Echtenacher B, Mannel DN. Lysis of tumor cells by natural killer cells in mice is impeded by platelets. Cancer Res 1999;59: 1295–300.
19. Sakakibara N, Gasa S, Kamio K, Makita A, Koyanagi T. Association of elevated sulfatides and sulfotransferase activities with human renal cell carcinoma. Cancer Res 1989;49:335–9.
20. Liu Y, Chen Y, Momin A, Shaner R, Wang E, Bowen NJ, et al. Elevation of sulfatides in ovarian cancer: an integrated transcriptomic and lipidomic analysis including tissue-imaging mass spectrometry. Mol Cancer 2010;9: 186.
21. Morichika H, Hamanaka Y, Tai T, Ishizuka I. Sulfatides as a predictive factor of lymph node metastasis in patients with colorectal adenocarcinoma. Cancer 1996;78:43–7.
22. Yoda Y, Gasa S, Makita A, Fujioka Y, Kikuchi Y, Hashimoto M, et al. Glycolipids in human lung carcinoma of histologically different types. J Natl Cancer Inst 1979;63:1153–60.
23. Suchanski J, Grzegrzolka J, Owczarek T, Pasikowski P, Piotrowska A, Kocbach B, et al. Sulfatide decreases the resistance to stress-induced apoptosis and increases P-selectin-mediated adhesion: a two-edged sword in breast cancer progression. Breast Cancer Res 2018;20:133.
24. Kobayashi T, Honke K, Gasa S, Kato N, Miyazaki T, Makita A, et al. Epidermal growth factor elevates the activity levels of glycolipid sulfotransferases in renal-cell-carcinoma cells. Int J Cancer 1993; 55:448–52.
25. Kobayashi T, Honke K, Gasa S, Miyazaki T, Tajima H, Matsumoto K, et al. Hepatocyte growth factor elevates the activity levels of glycolipid sulfotransferases in renal cell carcinoma cells. Eur J Biochem 1994;219:407–13.
26. Kobayashi T, Honke K, Gasa S, Imai S, Tanaka J, Miyazaki T, et al. Regulation of activity levels of glycolipid sulfotransferases by transforming growth factor alpha in renal cell carcinoma cells. Cancer Res 1993;53: 5638–42.
27. Gunaratnam L, Morley M, Franovic A, de Paulsen N, Mekhail K, Parolin DA, et al. Hypoxia inducible factor activates the transforming growth factor-alpha/epidermal growth factor receptor growth stimulatory pathway in VHL(-/-) renal cell carcinoma cells. J Biol Chem 2003;278: 44966–74.
28. Cao Q, Chen X, Wu X, Liao R, Huang P, Tan Y, et al. Inhibition of UGT8 suppresses basal-like breast cancer progression by attenuating sulfatide-alphaVbeta5 axis. J Exp Med 2018;215:1679–92.
29. Zhong Wu X, Honke K, Long Zhang Y, Liang Zha X, Taniguchi N. Lactosylsulfatide expression in hepatocellular carcinoma cells enhances cell adhesion to vitronectin and intrahepatic metastasis in nude mice. Int J Cancer 2004;110:504–10.
30. Gu L, Li H, Gao Y, Ma X, Chen L, Li X, et al. The association of platelet count with clinicopathological significance and prognosis in renal cell carcinoma: a systematic review and meta-analysis. PLoS One 2015;10: e0125538.
31. Haemmerle M, Stone RL, Menter DG, Afshar-Kharghan V, Sood AK. The platelet lifeline to cancer: challenges and opportunities. Cancer Cell 2018; 33:965–83.
32. Gasic GJ, Gasic TB, Stewart CC. Antimetastatic effects associated with platelet reduction. Proc Natl Acad Sci U S A 1968;61:46–52.
33. Takahashi T, Suzuki T. Role of sulfatide in normal and pathological cells and tissues. J Lipid Res 2012;53:1437–50.
34. Stettner P, Bourgeois S, Marsching C, Traykova-Brauch M, Porubsky S, Nordström V, et al. Sulfatides are required for renal adaptation to chronic metabolic acidosis. Proc Natl Acad Sci U S A 2013;110:9998–10003.
35. Aruffo A, Kolanus W, Walz G, Fredman P, Seed B. CD62/P-selectin recognition of myeloid and tumor cell sulfatides. Cell 1991;67: 35–44.
36. Kim YJ, Borsig L, Varki NM, Varki A. P-selectin deficiency attenuates tumor growth and metastasis. Proc Natl Acad Sci U S A 1998;95: 9325–30.
37. Data RE, Williams SB, Roberts DD, Gralnick HR. Platelets adhere to sulfatides by von Willebrand factor dependent and independent mechanisms. Thromb Haemost 1991;65: 581–7.
38. Cai QQ, Dong YW, Qi B, Shao XT, Wang R, Chen ZY, et al. BRD1-mediated acetylation promotes integrin alphaV gene expression via interaction with sulfatide. Mol Cancer Res 2018;16:610–22.
39. Weber MR, Zuka M, Lorger M, Tschan M, Torbett BE, Zijlstra A, et al. Activated tumor cell integrin alphavbeta3 cooperates with platelets to promote extravasation and metastasis from the blood stream. Thromb Res 2016;140:S27–36.